Analysis of electrodeless plasma source enhancement by an externally applied magnetic field for an inductive plasma thruster (IPT)

Conference Paper · October 2018

CITATIONS
4

READS
532

39 authors, including:

Silvia Masillo
University of Surrey
8 PUBLICATIONS **20** CITATIONS
SEE PROFILE

Francesco Romano
Universität Stuttgart
59 PUBLICATIONS **325** CITATIONS
SEE PROFILE

Ruggero Soglia
Politecnico di Milano
1 PUBLICATION **4** CITATIONS
SEE PROFILE

Georg Herdrich
Universität Stuttgart
526 PUBLICATIONS **3,002** CITATIONS
SEE PROFILE

Analysis of electrodeless plasma source enhancement by an externally applied magnetic field for an inductive plasma thruster (IPT)

Silvia Masillo[1*], Francesco Romano[1*], Ruggero Soglia[1], Georg Herdrich[1], Peter Roberts[2], Tony Schönherr[3], Tilman Binder[1], Adam Boxberger[1], Constantin Traub[1], Stefanos Fasoulas[1], Kate Smith[2], Steve Edmondson[2], Sarah Haigh[2], Nicholas Crisp[2], Vitor Toshiyuki Abrao Oiko[2], Rachel Lyons[2], Stephen D. Worrall[2], Sabrina Livadiotti[2], Jonathan Becedas[4], Gerardo Gonzalez[4], Rosa Maria Dominguez[4], Leonardo Ghizoni[5], Victor Jungnell[5], Kristian Bay[5], Jonas Morsbøl[5], Daniel Garcia-Almiñana[6], Silvia Rodriguez-Donaire[6], Miquel Sureda[6], Dhiren Kataria[7], Ron Outlaw[8], Rachel Villain[9], Jose Santiago Perez[9], Alexis Conte[9], Badia Belkouchi[9], Ameli Schwalber[10], Barbara Heißerer[10], Mirko Magarotto[11], Daniele Pavarin[11]

1 Institute of Space Systems (IRS): University of Stuttgart, Stuttgart, Germany
2 School of Mechanical, Aerospace and Civil Engineering, The University of Manchester, Manchester, UK.
3 ESA/ESTEC: European Space Agency (ESA), Noordwijk, The Netherlands
4 Elecnor Deimos Satellite Systems, Puertollano, Spain
5 GomSpace AS, Aalborg, Denmark
6 UPC-BarcelonaTECH, Terrassa, Spain
7 Mullard Space Science Laboratory, University College London, Holmbury St. Mary, Dorking, Surrey, UK
8 Christopher Newport University, Newport News, Virginia, US
9 Euroconsult, Paris, France
10 concentris research mamagement gmbh, Furstenfeldbruck, Germany
11 CISAS Center of Studies and Activities for Space, Università degli Studi di Padova, Padova, Italy

* s.masillo@surrey.ac.uk, romano@irs.uni-stuttgart.de

Abstract

Orbiting at lower orbital altitudes, where the residual atmosphere is source of aerodynamic drag requires an efficient drag-compensation system for satellite lifetime extension. One solution is proposed by using Atmosphere-Breathing Electric Propulsion (ABEP), a system that collects atmospheric particles and directly uses them as propellant for an electric thruster. Challenging is also the presence of reactive chemical species at low altitudes, such as atomic oxygen. This is an erosion source of (not only) the propulsion system components, i.e. acceleration grids, electrodes and discharge channels of conventional EP systems such as Radio frequency ion thrusters (RIT) and Hall-effect thrusters (HET). The thruster for an ABEP is proposed to be an Inductive Plasma Thruster (IPT) based on an electrodeless design. Hereby the first step is an efficient plasma source working on atmospheric propellant. Starting from IPG6-S as test-bed, a small scale inductively heated plasma generator at IRS [1]–[3], the mechanisms of RF power absorption by plasma in the low-pressure inductive discharges are analysed numerically and experimentally. The application of a relatively low external magnetic field is reported to enhance plasma density and power transfer efficiency [4]. Performances of both magnetized and unmagnetized plasma source, in terms of plasma resistance and density, are evaluated for different frequencies, input power, magnetic field intensity, pressure, temperature, plasma density profile, discharge channel and antenna dimensions. Investigations on plasma parameters such as its resistance R_P and the absorbed power, are based on numerical simulations and supported by theoretical and experimental results. In particular, the application of a magnetic field is foreseen to improve the coupling by increasing both R_P and absorbed power. A preliminary design of the plasma source for the IPT, currently under development, is also presented.

1. Introduction

The development of an electrodeless inductive plasma thruster (IPT) for an Atmosphere-Breathing Electric Propulsion system (ABEP) is currently under investigation at the Institute of Space System (IRS) of the University of Stuttgart [1] within the EU-funded Horizon 2020 DISCOVERER project, which aims at redesign Very Low Earth Orbit (VLEO) platforms [5]. Very Low Earth Orbits (VLEO) are relatively unexplored since, at these altitudes, the atmosphere creates significant drag to the spacecraft (S/C) and forces their orbit to early decay. However, VLEO might enlarge scientific and civil applications, Earth surveillance and observation and be economically advantageous for high data accuracy requirements. Indeed, mass and power budget of optical and radar payloads scale with the orbital height, for a given instrument performance. Within the EU-funded H2020 DISCOVERER project [5], key technologies for VLEO platforms are being developed. Merging the experiences in EP system development and atmospheric re-entry experimental campaigns with material-plasma interactions, the IRS is currently validating an EP system that enables sustained continuous flight at lower orbits. The proposed design is an ABEP-based electrodeless IPT. Challenges for such an ABEP system are also related to the decay of performances and lifetime of the thrusters due to electrode erosion, i.e. erosion of accelerating grids in RIT and of discharge channel in HET, without a magnetic shielding [6], and can be removed by an electrodeless design. For the IPT concept, the energy is transferred to the propellant without direct contact between the plasma and any electrode, and so is to be for the accelerating stage. IPG6-S is a small scale inductively heated plasma generator at the IRS facility (twin facilities are present at Baylor University [7] and Kentucky [8]), used as a first test-bed for the evaluation of its performances as an IPT operating on ABEP-related propellant. This plasma source was not designed as a propulsion device, but as a plasma source, whereas it serves to evaluate plasma discharge conditions with different propellants and mass flow rates. For the IPT, to reach high exhaust velocity and obtain enough thrust for drag compensation in an ABEP application, the design of both highly efficient plasma source and acceleration stage is required. Within this paper, conditions for the enhancement of RF power absorption by plasma are proposed with the goal to gain plasma source performances, in terms of ionization degree and plasma density, and, therefore, to properly design the IPT. Plasma power absorptivity is numerically investigated through HELIC code, developed by Arnush and Chen [9]–[11], and ADAMANT developed by Melazzi e Lancellotti at "Università degli studi di Padova"[12]. The simulations highlight the necessity to improve IPG6-S. On this purpose, the application of an external static magnetic field is foreseen to promote electromagnetic wave propagation in the discharge channel, allowing higher plasma density and ionization rate, also at low RF power range. An experimental test campaign has been performed to verify the enhancement of RF power absorption by plasma for the magnetised plasma source. Based on the simulated and tested conditions, a preliminary design for an IPT is proposed.

2. IPG6-S Facility

Extended testing has been performed by operating the inductively heated plasma generator IPG6-S with N_2, O_2, and CO_2 mixtures at IRS, according to atmosphere-breathing electric propulsion (ABEP) based system analysis[1]–[3], [13], [14]. IPG6-S is not designed for propulsion purposes. It is used to evaluate the plasma discharge behaviour with atmospheric propellants, and aids the design of a new plasma source. Aim of the new plasma source, that is already thruster oriented, is the development and test of an inductive plasma thruster (IPT) for ABEP application within the EU-funded DISCOVERER project. IPG6-S is an electrodeless device, a copper coil is wrapped around a quartz tube where the propellant flows, see Figure 1. The coil is fed by a RF power supply that operates, in the current configuration, at 3.3 MHz providing a maximum of anode current $I_{A,max}$ = 4 A, and a maximum input power of $P_{RF,max}$ = 15 kW. The current power supply is tetrode based. Therefore, the final frequency is determined by the impedance of the load together with the resonant circuit. IPG6-S is mounted on top of a 12 m^3 vacuum chamber, see Figure 2. It has a brass de Laval nozzle and it is water cooled. The main vacuum facility provides a base pressure of < 0.3 Pa without gas flow with a pumping speed from the central vacuum system of more than 250 000 m^3/h. A second vacuum pumping system composed by two oil diffusion pumps of 50000 l/min was not used for this test campaign, but it allows an even lower base pressure of < 10^{-6} Pa without gas flow.

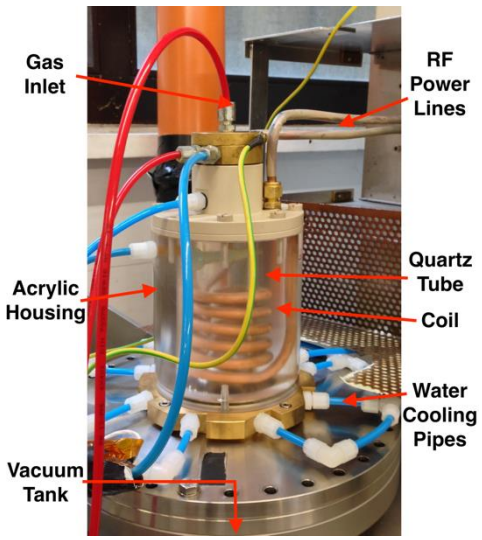

Figure 1. IPG6-S.

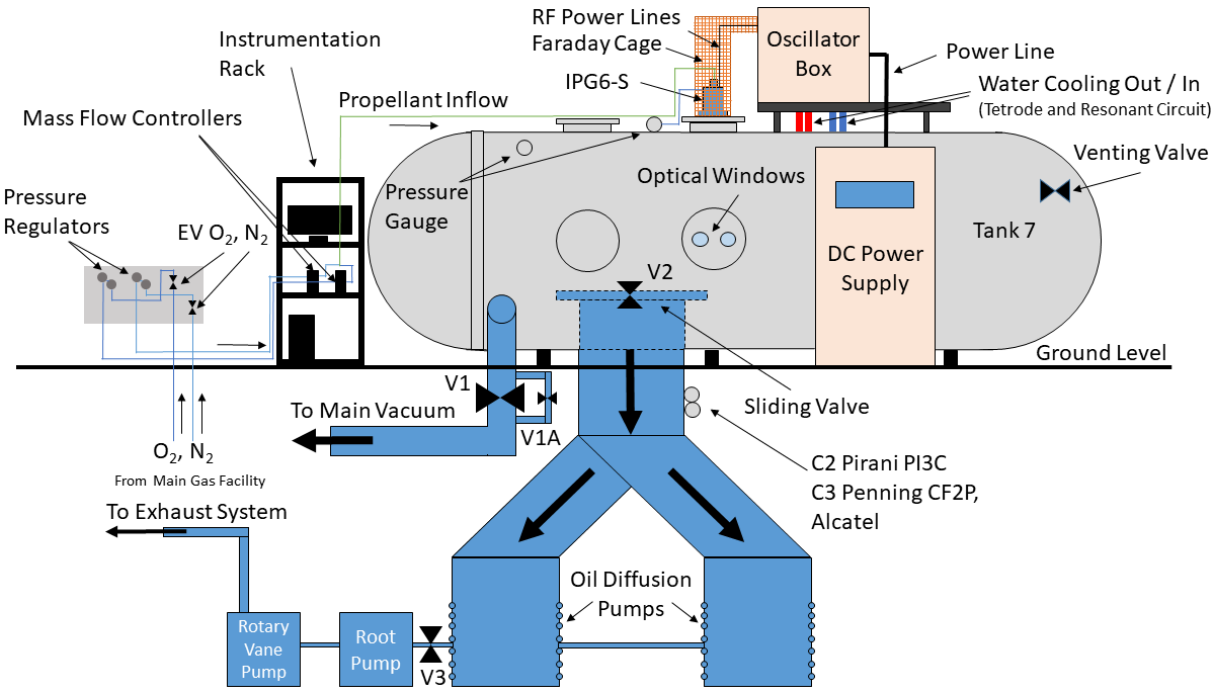

Figure 2. IPG6-S Test Facility.

3. Investigation of RF power absorption by plasma

The working principle of an IPG source is based on the generation and maintenance of the plasma discharge by means of electromagnetic fields, which couple to the electrons in the plasma and transfer energy to them to sustain the plasma. The efficiency of the power coupling between the power supply and the charged particles mainly depends on the design of the RF excitation. Precisely, the discharge can be generated by an axial ($\boldsymbol{E_z}$) or an azimuthal ($\boldsymbol{E_\varphi}$) E-field (the latter shown in Figure 3) and it corresponds to two different modes or regimes of the source: respectively, the electrostatic (E) or capacitive and the electromagnetic (H) or inductive mode. Commonly, the ICP source is ignited in E mode and undergoes E-H transition when the plasma density reaches a critical level as power in the coil is increased [4]. When the IPG source is placed in a static magnetic field, B_0, aligned with the symmetry axis, the mechanism of power absorption is influenced by propagating waves in the plasma. This is the so called W mode [4]. These disturbances, which are basically whistler waves confined to a cylinder moving from the antenna to the plasma bulk, are able to ionize the gas deeply into the discharge and produce density > 10^{19} m^{-3} [15]. More recently, the importance of Trivelpiece-Gould (TG) waves has been also demonstrated [9]. The latter are electron cyclotron wave traveling obliquely to the B-field, generated near the inner wall to satisfy the boundary conditions on the cylinder.

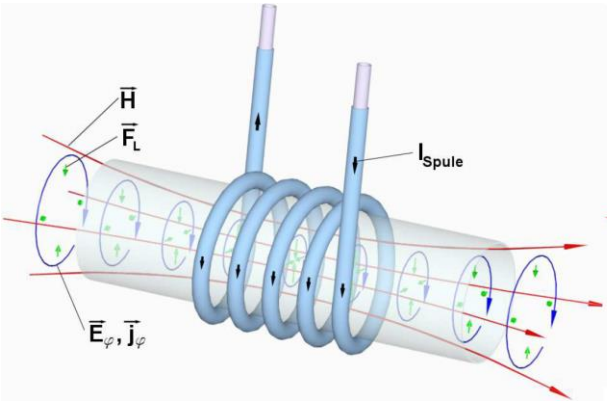

Figure 3. Electromagnetic fields generated in inductive mode[16].

Thomson, in [17], described the purely-inductive discharge as a transformer, consisting of two windings, representative of the coil and the plasma, interlinked by a mutual inductance M. By applying the transformer model to purely inductive coupled discharges, it can been demonstrated [4] that the active power absorbed in the plasma, P_p, is proportional to the square of the active current flowing through the antenna, I_{RF}, as in Eq. (1):

$$P_p = \frac{1}{2} R_p |\widetilde{I_{RF}^2}|. \quad (1)$$

And it is also related to the total active RF input power, P_{in}, as in Eq. (2)

$$P_{in} = P_{RF} \frac{Rp}{(R_p + R_c)}, \quad (2)$$

where R_c is the effective circuit resistance and R_p is the plasma resistance.

Since P_p is proportional to R_p, see Eq. (1), an enhancement of RF power absorption is obtained if R_p is increased. With R_p much larger that R_c, the input RF power is coupled with the plasma and only a fraction is lost in the antenna and the circuit [18]. To determine the factors that mainly influence the RF power transfer efficiency in purely inductive mode, R_p, is numerically

computed for different antenna and discharge channel shapes, operating frequencies, f_{RF}, neutral gas pressures, p, collisional factors, ν, electron temperatures, T_e, plasma density profiles, $n(r)$, and static magnetic field intensities, B_0. In particular, R_p is analysed through the HELIC code, a C^{++} program based on the theory developed by D. Arnush and F.F. Chen between 1997 and 2000 [9]–[11]. HELIC solves a set of four coupled radial differential equations derived from the Maxwell's equations for a radially non uniform cold-plasma. A model of the IPG6-S has been developed in HELIC as a closed cylindrical discharge channel with a helical RF antenna. The input geometrical parameters are presented in Table 1.

In particular:

- Cavity radius, c, and length, LC, are taken large enough to do not influence the analyses;
- Plasma radius, a, has the same radius of IPG6-S discharge channel inner diameter and it is assumed to be axisymmetric;
- Working frequency, f, is based on the previous experimental campaign at the IRS [1];
- Antenna radius, b, is calculated as the sum of the plasma radius, a, the thickness of the discharge tube and the radius of the antenna wire of the IPG6-S;
- Antenna is located at the extremity of the discharge channel. The position is calculated as in Eq. (3):

$$ZA = -\left(\frac{LC}{2} - \left(LD - \frac{LA}{2}\right)\right) \tag{3}$$

Table 1. Plasma source IPG6-S input parameters in HELIC.

Parameter	Symbol	Value
Plasma radius	a	0.0185 m
Antenna radius	b	0.0215 m
Cavitii radius	c	0.2 m
Ion	ion	Ar
Frequency	f	3.3e+06 Hz
Azimuthal mode	m	+1
Antenna type	-	t-turn Helix (m odd)
Turns	-	5
Antenna length	LA	0.08 m
Cavity type	-	Bounded
Cavity length	LC	2 m
Image sign	ei	+1 (insulating endplate)
Antenna distance from centre	ZA	-0.86 m

The ions species, implemented in the code, are H_2, He, Ne, Ar and N_2. If B_0 is set to ≈ 1, HELIC evaluates the ICP source field, while for higher values, the W-mode is taken into account. Plasma creation and transport are not evaluated. The absorption of RF energy dominated by mode conversion to heavily damped TG modes at the radial surface is considered.

The code is requested to evaluate R_p and the radial power absorbed, $P(r)$, for a given range of plasma density ($10^{16}m^{-3}$ - $10^{19}m^{-3}$), according to those reached by IPGs in literature [19].

The main results of the analyses are hereby summarized:

- R_p increases with the frequency, whereas an asymptotic trend is found for f > 27.12 MHz. The trend has been related to the decrease of the skin depth with the increase of the frequency;
- R_p increases with the antenna diameter and the lower the displacement between antenna and discharge channel is, the higher the coupling efficiency is. This also confirms previous experimental investigations at IRS [20];
- R_p highest values are for the helical-type antenna;
- R_p strongly depends on the plasma parameters, in particular, for a given plasma density, a greater R_p is obtained by increasing ν , p and T_e, confirming that RF power absorption in a unmagnetized plasma is mainly governed by collisional mechanisms;
- RF power is coupled and absorbed by plasma only in the skin layer. The higher the plasma density close to the inner wall of the discharge channel, the higher is R_P.

In Figure 4 a comparison between the design of the original plasma source, IPG6-S, and a design optimised according to the highest achievable R_p and based on the simulations is reported. In particular, for the same plasma parameters (ionising gas, plasma density, plasma density profile, collisional factor, electron temperature and neutral gas pressure) a 5-turns helical-type antenna has been selected for both plasma sources. Then, R_p is increased by enlarging antenna and discharge channel diameter, antenna length and working frequency. Despite the remarkable difference in terms of R_p between the two plasma sources, if low neutral pressure and low electron temperature are simulated in a non-uniform plasma density profile, for the same plasma density, R_p is highly attenuated, as shown by the dashed line in Figure 4. Precisely, the case here reported refers to a centred-peak plasma density profile and neutral pressure of $p = 0.133\ Pa$, working frequency is 40.68MHz, ionising gas is Ar.

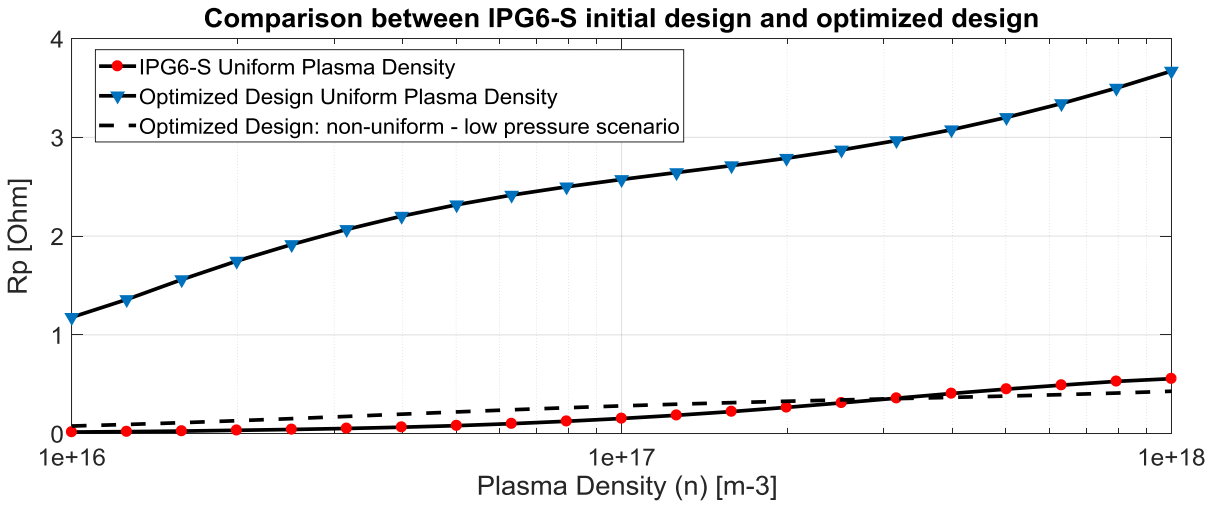

Figure 4. Plasma source design comparison: IPG6-S at 3.3 MHz, Ar, p=1.33 Pa, uniform plasma density profile (red dots line); Optimized design at 40.68 MHz, Ar, p=1.33Pa, uniform plasma density profile (blue triangles line); Optimized design at 40.68MHz, Ar, p=0.133 Pa, centred-peak plasma density profile.

To further improve the IPG6-S, an investigation of the dependence of RF power absorption in magnetized plasmas is done. The simulations consider a range of B_0 between 0.01 T and 0.1 T, different antennas, p, T_e and $n(r)$. The operating frequency is fixed at f = 40.68 MHz.

The overall results for the magnetised source analyses are hereby summarized:

- R_p shows almost the same response to the geometrical dimensions of the antenna and the discharge channel for unmagnetized and magnetized plasma. Nevertheless, the resulting R_p values are one order of magnitude higher if B_0 is applied;
- A common trend for R_p is to increase to a maximum, then to rapidly decrease. For higher B_0, the peak moves toward higher plasma density. According to [9], the low-field peak can be caused by wave reflection from the boundaries or due to a resonance between the whistler waves that takes part in the discharge channel in a magnetic field.
- R_p is almost independent on both ν and T_e, its highest values are obtained for lower pressure of the neutral gas. Precisely, the analyses refer to the following ranges: $\nu = 1$ - 6; T_e = 3 - 6eV; p=0.013 Pa - 1.33Pa;
- R_p maxima are observed for centred-peak plasma density profile and the density width, representative of the plasma density close to the inner wall of the discharge channel, has a minor impact on R_p in comparison to the unmagnetized plasma.
- Power absorption is not limited to the skin layer but the RF field is able to penetrate the plasma. The absorptivity strongly depends on the plasma density and plasma density profile.

The radial power absorption $P(r)$, for the unmagnetized (Figure 5) and magnetized plasma (Figure 6 - Figure 7), is evaluated at $n = 10^{18} m^{-3}$ considering different $n(r)$. $P(r)$ is plotted over r/a, where a is the discharge channel radius and r the distance measured from the centre of the discharge. Similar results have been recorded by [21] and [22]. The explanation for different radial power coupling distribution for the magnetized plasmas may be related to the presence of waves propagating into the discharge. Since TG modes tend to be localised in the thin layer near the surface, they are also the principal responsible of power coupling to the plasma in the magnetised sources [23].

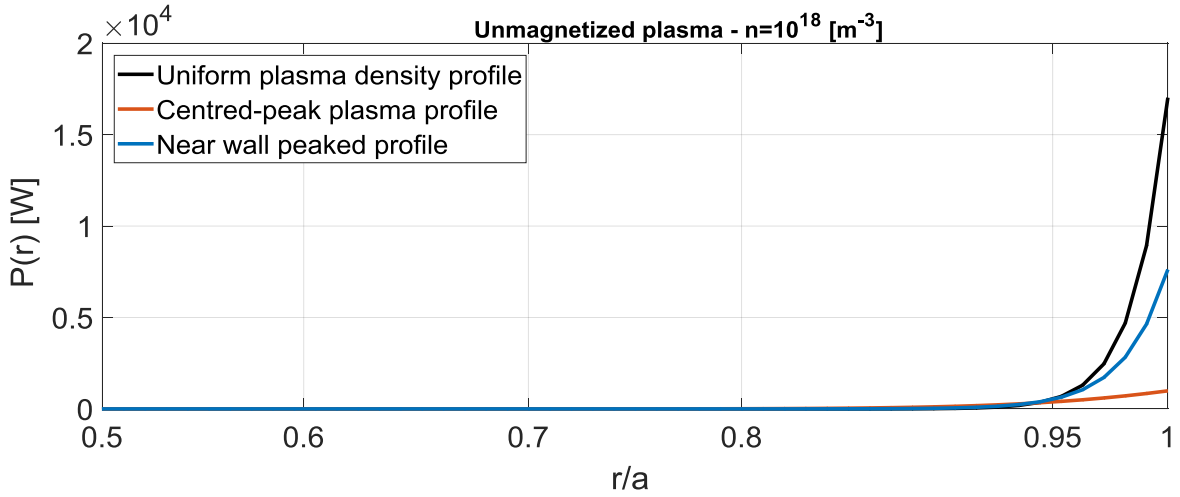

Figure 5. P(r) absorption profile: unmagnetized plasma source – different plasma profiles; Ar, f=40.68 MHz.

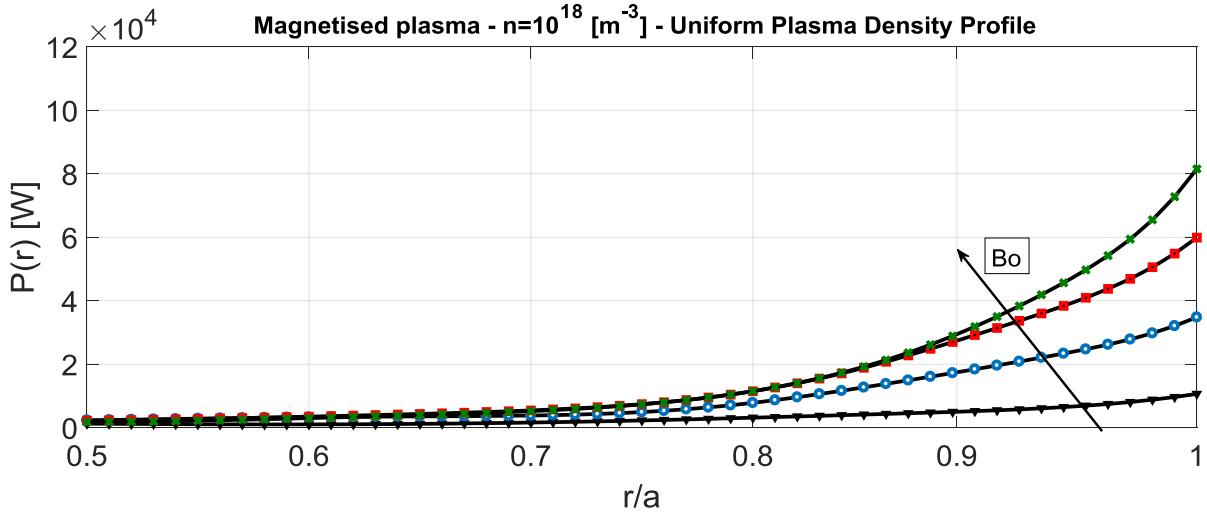

Figure 6. Radial power absorption profile: magnetised plasma – uniform plasma profile; Ar, f=40.68 MHz, B_0=0.01-0.1 T.

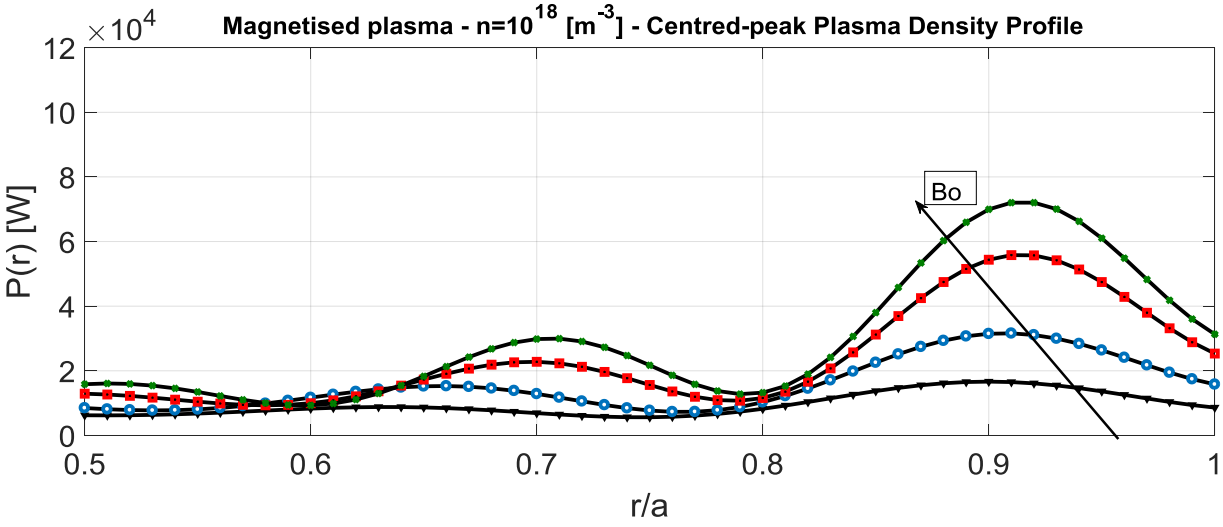

Figure 7. Radial power absorption profile: magnetised plasma – centred-peak plasma profile; Ar, f=40.68 MHz, B_0=0.01-0.1 T.

These analyses are useful to understand the parameters that mostly affect the plasma power absorptivity. However, their validation is still necessary e.g. to assess the potential impact to the efficiency of a later optimized plasma source or inductive propulsion system. This is made within an experimental campaign and the use of a software able to evaluate antenna geometry and its influence on the power deposition in the plasma source. In fact, plasma absorptivity greatly depends on the reactive and active components of the input RF power, and on the geometrical and electrical parameters of the electrical circuit. ADAMANT (Advanced coDe for Anisotropic Media and ANTennas) [12] is a full-wave numerical tool developed for the study of wave propagation and for the design and optimization of plasma antennas. ADAMANT has been available thanks to a collaboration established between IRS and "Università degli Studi di Padova", in Italy. Contrary to HELIC code that considers the antenna as an infinitely thin layer and normalises R_p to I_{RF}=1A, in ADAMANT the RF power absorbed by plasma is evaluated by modelling a plasma column and an RF antenna. The antenna is

assumed to be a perfect electric conductor (PEC). A voltage gap generator, set by an input voltage at the circuit port, produces the excitation mode. To analyse the mechanisms of power absorption by plasma through the ADAMANT code, two helical-type antennas, respectively 50 mm and 80 mm long, have been designed. Precisely, considering a copper wire of external diameter of 10 mm, and working frequency of 40.68 MHz, the two antennas have as requirement that the impedance load is lower than 50 Ω. This to fit with the requirement of the recently acquired auto-matching network for the power supply of IPT. Instead, plasma is simulated as a cylinder 180 mm long and with a diameter of 37 mm, in agreement with the dimension of the IPG6-S discharge channel.

From a comparison between the two tools, it results that:

- The codes are able to estimate the response of the absorbed power, P_p, on the plasma parameters. Precisely, in the case of unmagnetized sources, both codes predict an increase of the power coupling efficiency for a higher p and T_e. When the magnetised plasma source is considered, a decreasing trend of P_p with rising of p and an almost independent behaviour on T_e is confirmed. In the current available version of ADAMANT, the plasma density profile is uniform. By latest December 2018, a second version will be available at IRS and will allow to validate HELIC results based on different radial plasma density profiles.
- HELIC calculates the absorbed power by evaluating the plasma resistance, R_p, for a normalised input current of 1 A and its adaption to plasma parameters. For the design of the RF excitation mode of the IPT, the antenna parameters and their influences on the reactive and active components of P_p have to be investigated. While ADAMANT calculates the current distribution over the surface of the antenna given the voltage gap input and the response of the plasma.

The outcome from ADAMANT simulations is the dependence of P_p on B_0, depending on antenna type and plasma conditions. Precisely, in HELIC, R_p maxima further increase and move to higher n when a greater B_0 is applied, as shown in Figure 8. This is accounted in almost all the plasma conditions analysed. The behaviour is different if the antenna impedance is taken into account. Simulations in ADAMANT have demonstrated that the application of a higher B_0 has not always a beneficial impact on the plasma absorptivity. Indeed, early results have showed asymptotic or dropping trends of $P_p(B_0)$ under particular conditions, as the one presented in Figure 9. Here, a range of B_0 between 0-0.04 T is applied to a 2-turns helical-type antenna, 50 mm long and with a core diameter of 37 mm. In comparison to $B_0 = 0.02\ T, P_p$ drops if B_0 is amplified.

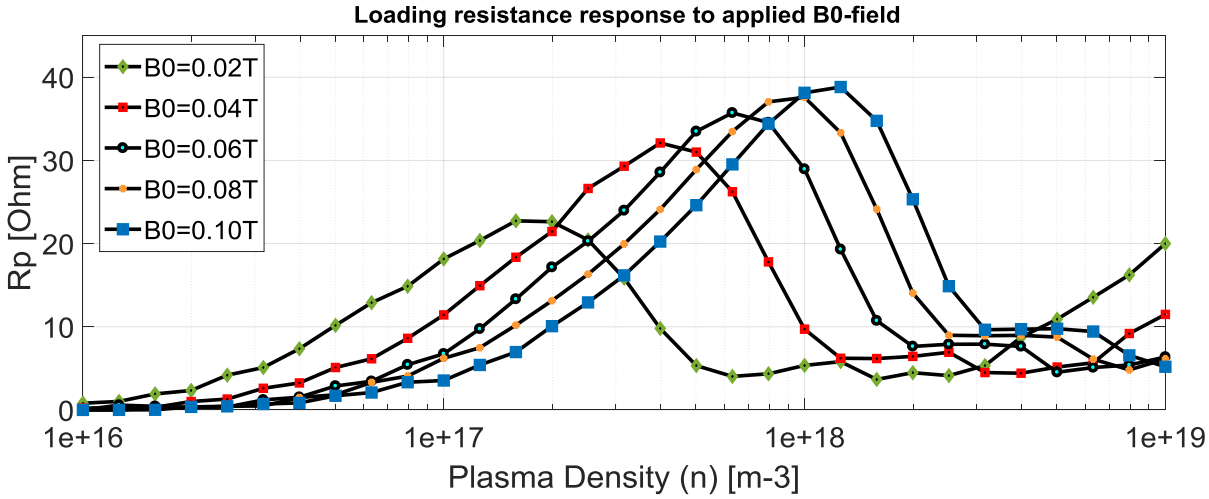

Figure 8. HELIC simulations: loading resistance response to applied B_0-field; Ar, f=40.68 MHz, B_0=0.02-0.1 T.

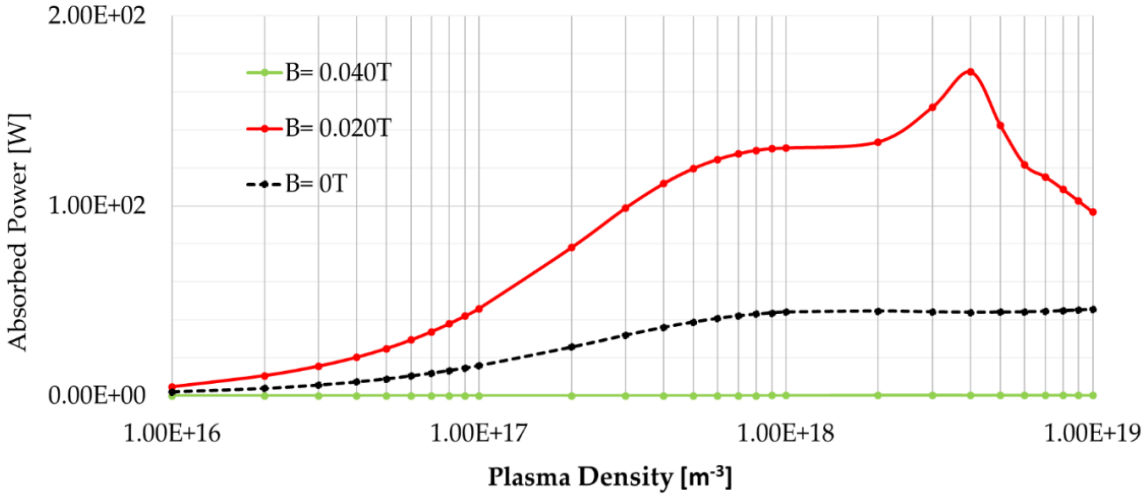

Figure 9. ADAMANT simulations: plasma absorbed power at zero B_0-field and to applied B_0-field (B_0=0.02 T and 0.04 T); Ar, f=40.68 MHz.

To further analyse the conditions simulated by ADAMANT and HELIC, IPG6-S has been modified with the installation of an electromagnet (EM), as presented in Section **Error! Reference source not found.**. The design of the EM gives a certain level of flexibility regarding the intensity of the magnetic field. Since B_0 can be varied according to the DC current flowing into the wires, IPG6-S can be tested in various conditions.

4. Electromagnet Design (EM)

Simulations done with HELIC and ADAMANT have showed the enhancement of plasma density and power transfer efficiency for an applied B-field with intensity between 0.005 – 0.07 T. Therefore, an EM has been accordingly designed, built, and mounted around IPG6-S. The EM, shown in **Error! Reference source not found.**, is a solenoid consisting of about 800 windings of a magnetic wire for a total resistance of 4 Ω at ambient temperature. Its design is mainly driven by the available power supply, TCR 160T15 by Electronic Measurements, for which maximum direct current and voltage are, respectively, 15 A and 60 V.

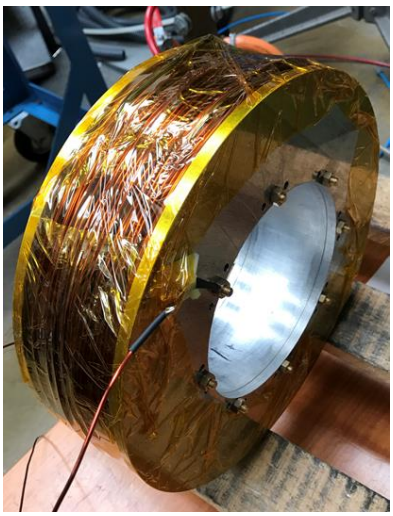

Figure 10. Electromagnet.

Due to the presence of the cooling water pipes of the IPG6-S, the maximum available height for the EM housing is 110 mm and the minimum possible diameter is 160 mm. The EM structure has been manufactured with two aluminium plates (internal diameter 160 mm, external diameter 300 mm) and an aluminium hollow cylinder (internal diameter 160, external diameter 180 mm). A copper wire of 600 meters, with a diameter of 2 mm (2.107 mm considering the insulation) has been wrapped around the structure.

The total mass of the EM is around 20 kg. It has been tested before being mounted on IPG6-S to ensure that no overheating occurs during the operation, since the insulation of the copper wire can withstand up to 200 °C. After a 30 min test with a DC current of 10 A, the maximum temperature reached by the EM was 62 °C.

A magnetic field model of IPG6-S assembled with the EM is simulated using the software FEMM 4.2. FEMM is a software for solving low frequency electromagnetic problems on two-dimensional planar and axisymmetric domains. It solves linear/nonlinear magnetostatic problems, linear/nonlinear time harmonic magnetic problems, linear electrostatic problems, and steady-state heat flow problems [24]. The IPG6-S and EM assembly, simulated as in Figure 11, is made by one single electromagnet, with 800 turns of copper wire with 2 mm diameter. The EM has an internal diameter of 160 mm and an external diameter of 300 mm and a height of 70 mm. In particular, Figure 11 shows a sectional view of the simulated EM placed around the IPG6-S and fed with 10 A of DC current. The B-field intensity is evaluated along the discharge channel (see red line in Figure 11) and results are plotted in Figure 12 for different values of DC. B-field intensity is between 0.005 T and 0.07 T, for a DC current between 1 A and 15 A, and slightly decreases as one moves from the inlet of the discharge channel (bottom in Figure 11) to the outlet. This determines a slightly diverging magnetic field to push the ionized gas out of the discharge channel by the effect of Lorentz force.

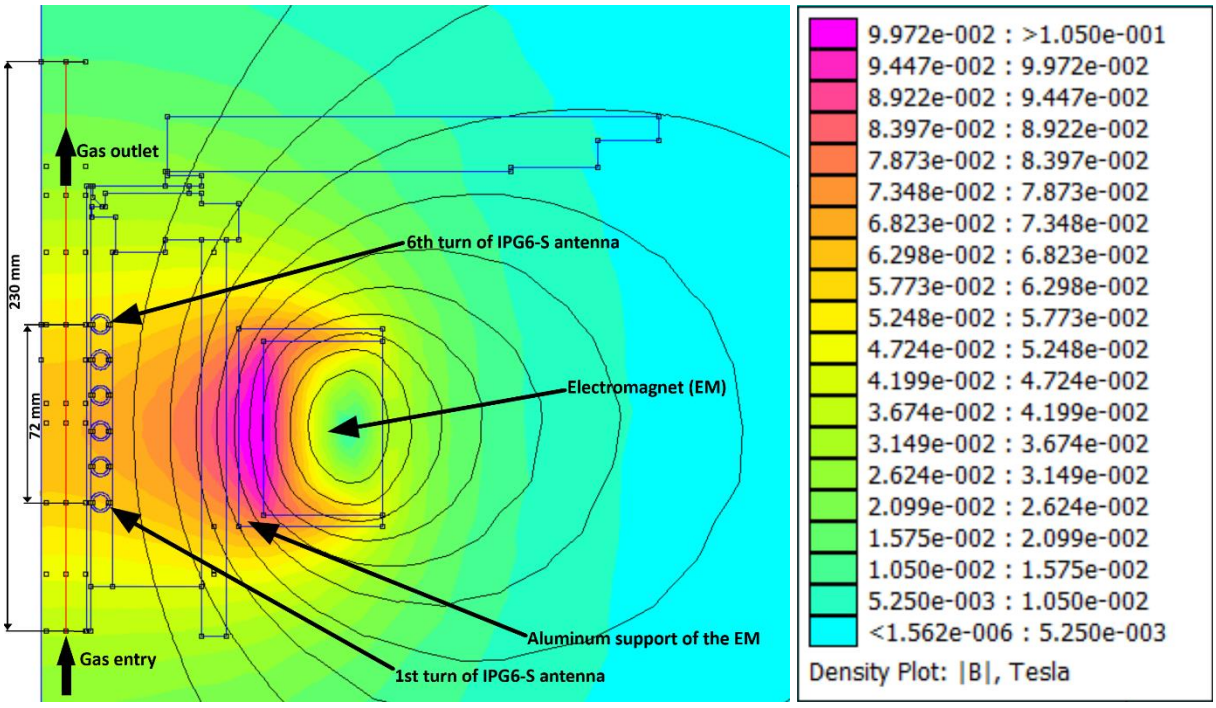

Figure 11. FEMM 4.2 simulation of EM assembled around IPG6-S: B-field is evaluated along the red line.

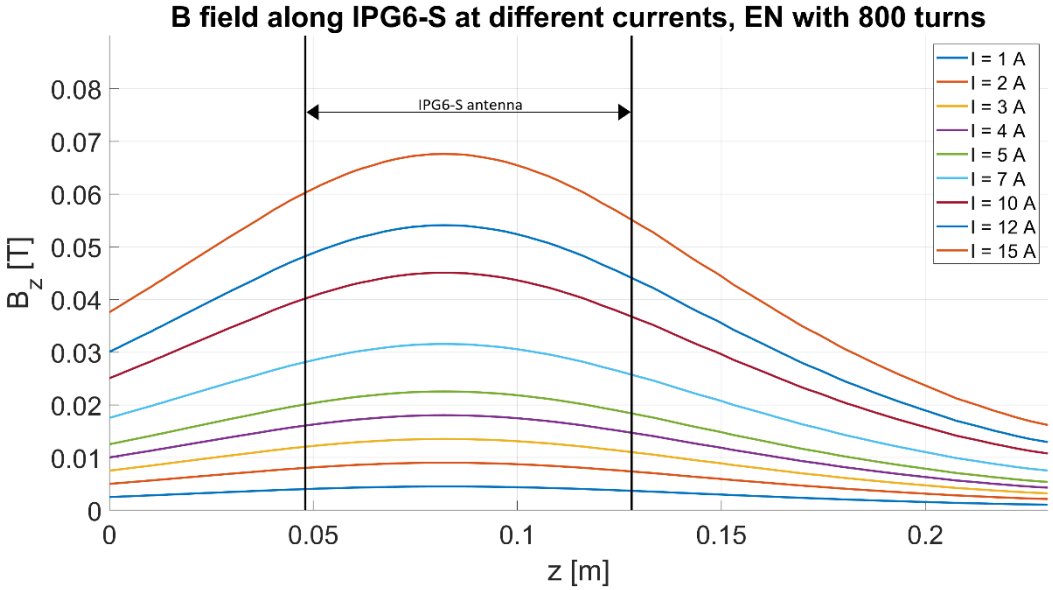

Figure 12. B-field generated by the electromagnet in the central region of the IPG6-S discharge channel for different current.

5. Experimental campaign

During the experimental campaign, IPG6-S has been used as test-bed to investigate the influence of externally applied B-field on the discharge channel.
IPG6-S is mounted on a flange on the top of the vacuum chamber (Figure 2) and the plasma is directed downward. A window provides optical access to the plasma plume ejecting the nozzle. The electrical power for the IPG6-S is provided by the RF generator Himmelwerk HGL 20-4B, with a maximum input power of 15 kW at the frequency of 3.3 MHz. The active power P_{RF} is manually regulated in the control panel. The EM is fed by the DC power supply TCR 160T15 from Electronic Measurements, to provide DC current, I_{EM}, in the range 0-15 A, as previously presented in Sec. 4. The working gases used for the experimental campaign are $N_{2,}O_2$ and Ar, injected at different mass flow rates. In particular, Ar ranges from 1.38mg/s to 17.88mg/s; O_2 from 0.06mg/s to 4.35mg/s; N_2 from 0.87mg/s to 4.64mg/s, according to the test facility capabilities.
The following conditions have been tested:

- Plasma ignition without applied magnetic field;
- Plasma ignition with applied magnetic field;
- Saturation of the active power with applied magnetic field;
- Reduction of reflected power by means of I_{EM} and P_{RF} tuning;
- Variation of the mass flow rate for constant I_{EM} and P_{RF};
- Plasma hysteresis.

As shown in Figure 13 - Figure 17, data are analysed by comparison of the variation of the power absorbed by plasma, P_{RF}, together with the anode current of the power supply, I_A, the injector pressure, p_{inj}, and the cooling power of the discharge channel, $P_{gen,cooling}$, evaluated as change of water temperature in the generator cooling system. The EM data are superimposed on the graphs.
Through the experimental test campaign, it has been observed that:

- At the lowest gas flow rate, plasma ignition could not be achieved without aid of the EM;
- In almost all the cases, a sudden jump of P_{RF} has been recorded as soon as the EM was switched on. Relatively low magnetic fluxes were required: 5.4-11.5 mT;
- The increase of P_{RF} is not linearly related to B_0. There is a saturation point after which a higher applied B-field does not influence a further enhancement of the power absorptivity, whereas it has an impact on the confinement of the plasma plume (the latter is a result of visual inspection during the experiments);
- A reduction of reflected power is possible, corresponding to a reduction of the oscillations of the P_{RF} signal by tuning the EM until a matching condition is reached;
- The power jump associated to the EM activation is usually associated to an increase of inner tube pressure p_{inj};
- Change in brightness and shape of the plasma plume are visually observed trough the tank window;
- The experiments could be replicated in almost all the cases and a hysteresis of the plasma has not been observed.

In the following, results of the test campaign are presented and briefly analysed. Figure 13 - Figure 17 present $P_{RF}, P_{gen,cooling}, p_{inj}$ and I_A recorded during tests. On the x-axis, the duration of the test in seconds is reported. Since only singular conditions are here reported, the x-axis has an arbitrary range. On the y-axis $P_{RF}, P_{gen,cooling}, p_{inj}$ and I_A are shown; p_{inj} and I_A are scalar multiplied by a value of 100 for an easier reading of the plots.

Figure 13 shows the test performed on N_2 at $\dot{m} = 1.29\ \frac{mg}{s}$. At this mass flow rate, p_{inj} is almost at the minimum allowable and plasma ignites at $I_A = 1.8\ A$ (t~520 s), but P_{RF} is low in comparison to the applied-B_0 conditions. Precisely, at $B_0 = 5.4\ mT$, a P_{RF} jump from 600 to 1000 W has been observed. P_{RF} further increases up to 1800 W by increasing B_0 up to 13.6 mT. The increase of B_0-field corresponds also to a greater noise in the P_{RF} signal due to an increase of the reflected power. The active component of P_{RF} has reached a maximum at about 3 kW for B_0~22.2 mT. A change of the plasma plume brightness and length has been also observed as shown in Figure 14.

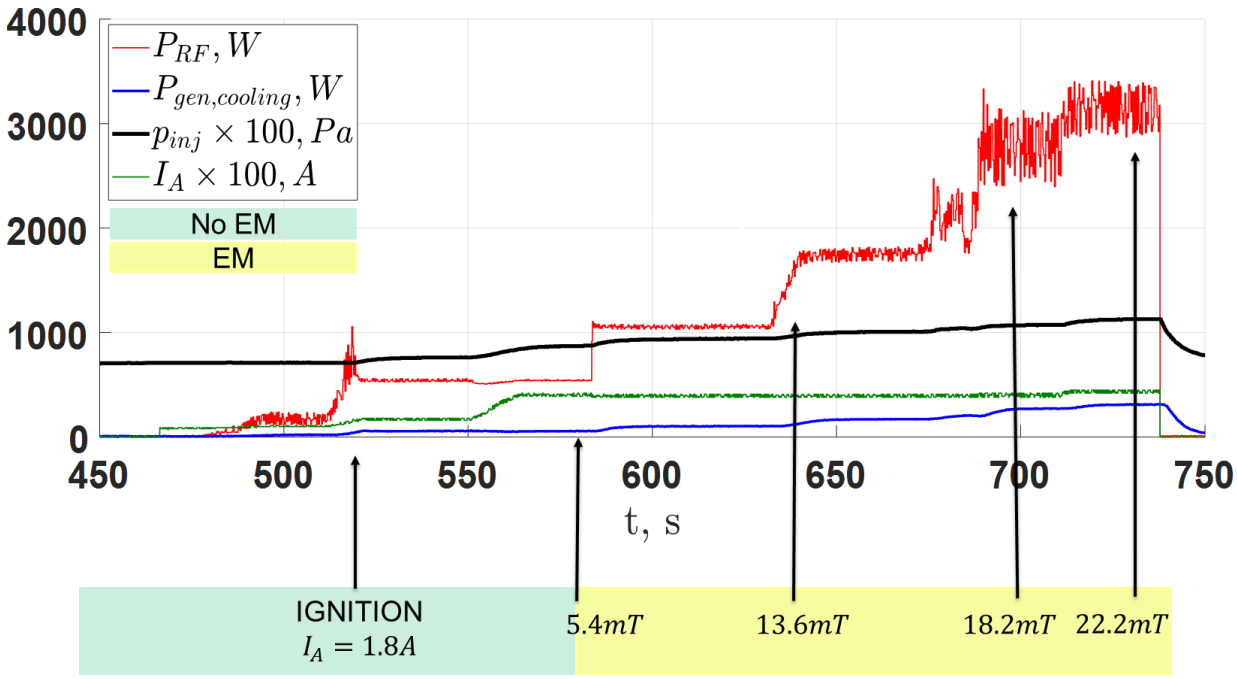

Figure 13. IPG6-S test: N_2 at 1.29 mg/s, $p_{inj} = 7.1\ Pa, p_{tank} = 0.5\ Pa$ [13].

Figure 14. IPG6-S test: N_2 1.29 mg/s - Change of plasma plume diffusivity and brightness for increasing applied B_0-field.

Figure 15 presents the results for Ar with a mass flow rate of 1.38 mg/s, which corresponds to the minimum allowable p_{inj}. Compared to N_2, at this mass flow rate, or lower, plasma ignition was not possible, even if the maximum I_A of 4 A was fed to the coil. Contrary, by applying a B_0-field of 11.3 mT, at $I_A = 1.8\,A$, the plasma ignited even if P_{RF} is considerably low (P_{RF}~500 W). P_{RF} ~1 kW is recorded for a B_0 =66.5 mT and further increase of I_A brings to a singular effect of a "switch off" of the plasma: at 1020 s, the plasma plume was not visible anymore, whereas the average values I_A was unchanged. Similar conditions were observed within ADAMANT simulations, as in Figure 9, where the active component of the active power suddenly drops of two orders of magnitude by increasing the B_0 from 20 mT to 40 mT. The phenomena in Figure 16 could be related to antenna coil-B-field "un"matching conditions, but further investigations are needed to prove the statement.

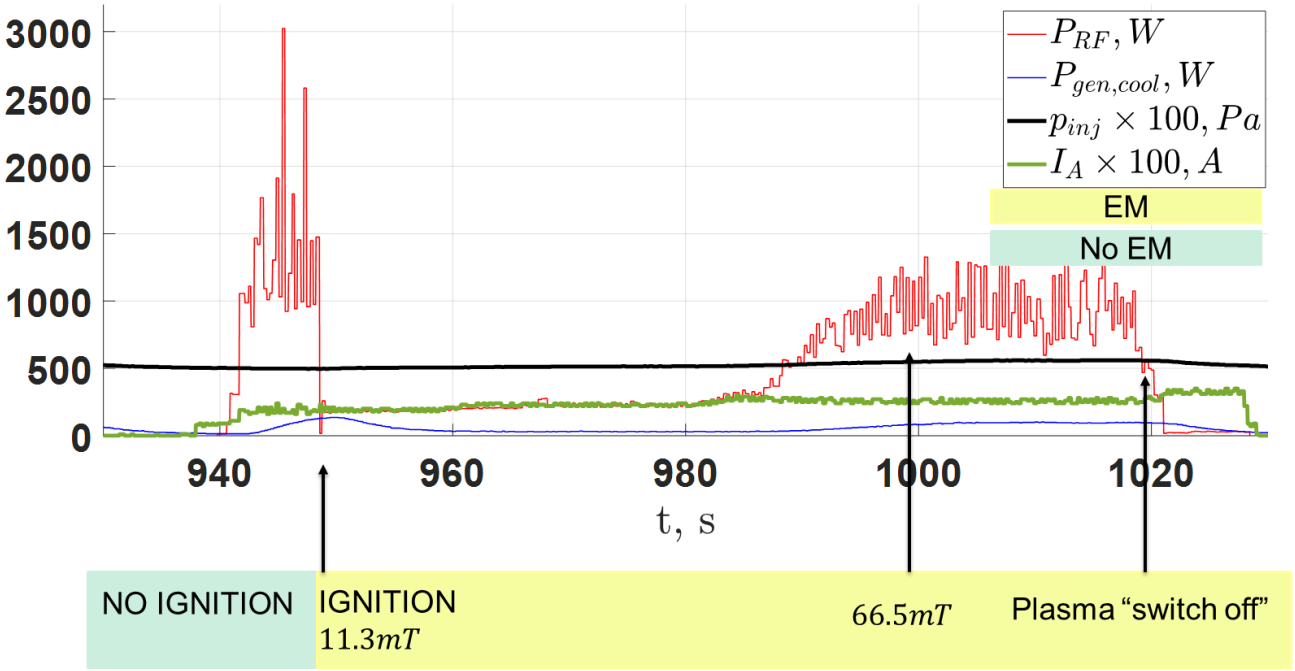

Figure 15. IPG6-S test: Ar at 1.38mg/s, $p_{inj} = 4.96\ Pa, p_{tank} = 0.31\ Pa$ [13].

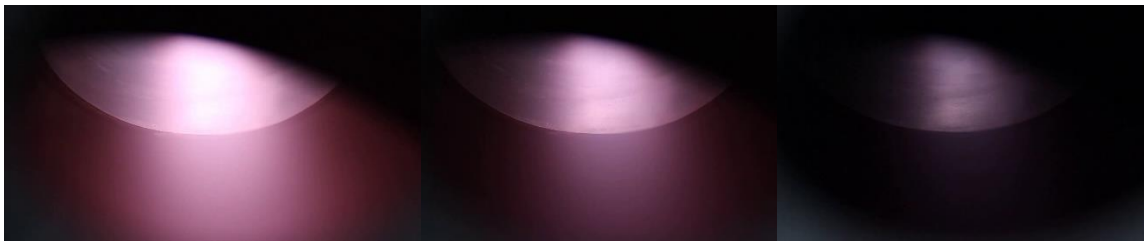

Figure 16. IPG6-S test: Ar at 1.38mg/s - plasma "switch off" condition with increasing B_0.

Figure 17 shows experiments for O_2 at $\dot{m} = 4.36\frac{mg}{s}$, which corresponds to the maximum allowable mass flow rate for O_2. In this case, the highest P_{RF} and relative jump has been observed. The EM has been always switched-on and B_0 intensity increased from 5 to 60 mT. Plasma ignited at $B_0 = 5\ mT$ and I_A =1.9 A. The best matching condition, for which the

reflected power is almost null corresponding to almost no noise on P_{RF} signal, has been found by tuning the EM and the RF generator accordingly. At $\dot{m} = 4.36\ mg/s$, a matching condition corresponds to $B_0 = 6.8\ mT$ and $I_A = 1.8\ A$. An increase of B_0 −field caused a P_{RF} jump of more than 2.5 kW for the same I_A. The intensity and the shape of the plasma plume were remarkably different before and after the jump. Together with the information on p_{inj}, that has almost triplicated, the assumption that the discharge could have reached an E-H transition can be done. To confirm the inductive discharge conditions, further investigations based on plasma diagnostics are necessary.

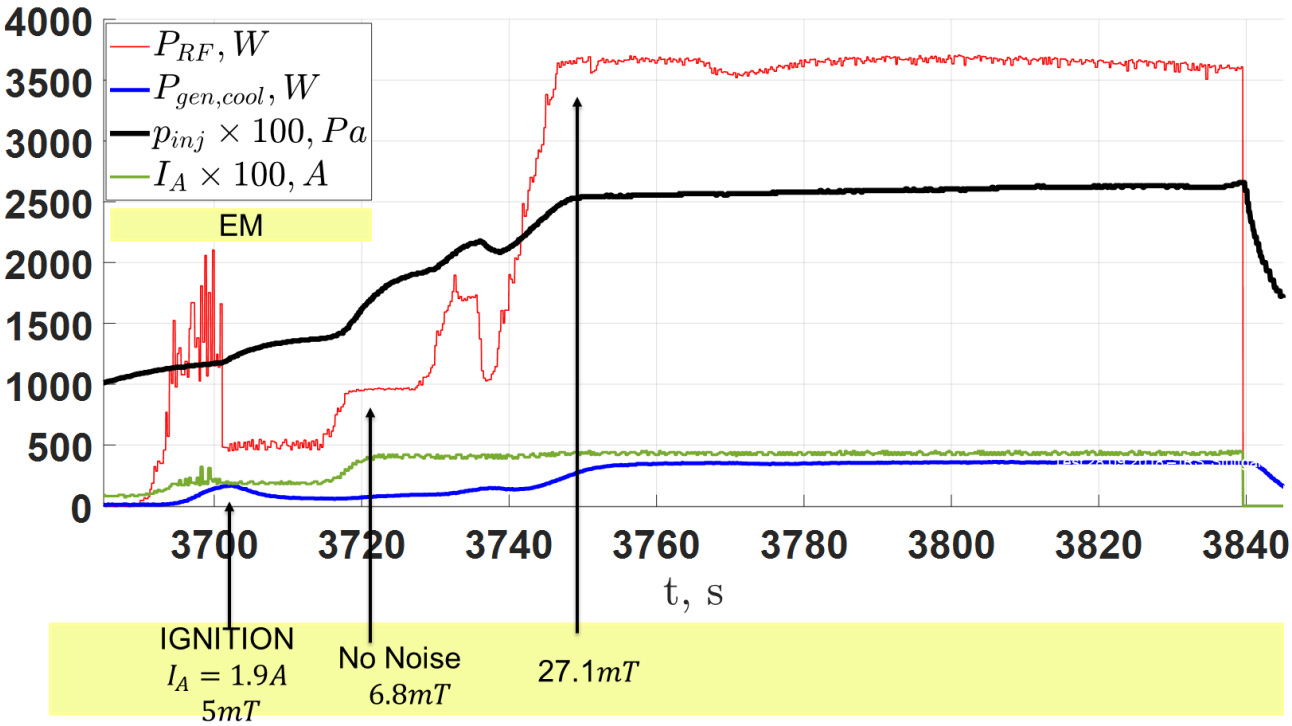

Figure 17. IPG6-S test: O_2 at 4.36 mg/s, $p_{inj} = 13.63\ Pa, p_{tank} = 0.42\ Pa$ [13].

Figure 18. IPG6-S test: O_2 at 4.36mg/s - Change of plasma plume diffusivity and brightness for increasing applied B_0-field.

6. Scaling of IPG6-S to IPT

ADAMANT and HELIC simulations, and the experimental campaign, have shown that an enhancement of RF power absorption by plasma with an externally applied DC magnetic field is achieved. At the same time, it has been shown that the RF power absorptivity highly depends on the plasma conditions that, within the framework of this paper, have been evaluated according to literature [4], [21]. A direct calculation could only be possible by the use of further plasma diagnostics that enable the assessment of all relevant input parameters for the numerical tools. For this purpose, the future IPT is to be installed to a new facility set-up that is currently under completion at IRS, and expected to operated for the first time in early 2019. The new facility set-up will be completed with the following plasma diagnostics:

- Retarding potential analyser (RPA);
- Langmuir probe;
- Faraday probe;
- Optical Emission Spectroscopy (OES);
- Laser Induced Fluorescence (LIF);
- Mach Zehnder Interferometer (MZI);
- Tuneable Diode Laser Absorption Spectroscopy (TDLAS).

The vacuum system for this facility is able to provide a base pressure down to $10^{-5}\,Pa$ and will be provided with a gas feeding system that will operate in the gas flow range of $\dot{m}$ between 50 $\mu g/s$ and 1 mg/s of Ar, N_2, O_2, CO_2 and mixtures.

Concurrently, a first prototype for IPT has been designed and almost completely assembled [13]. This device is the first step toward the final IPT, passively cooled, and optimised for a power range of 0.5-5.5 kW and most suitable for ABEP-relevant mass flow rates [1]. A preliminary design is based on the same discharge channel dimensions of the IPG6-S, a quartz tube of outer diameter of 40 mm and length 180 mm. The IPT is designed in such a way that the discharge channel length can be modified, as the gas injector can be moved along the axis of the discharge channel. Moreover, the injector provides a swirling direction to the injected gas for a better plasma stabilisation [16]. To provide the maximum flexibility, the EM position can be adjusted along the direction of the discharge channel. The EM has been previously designed to be compatible to both IPG6-S and IPT, in terms of geometry and B-field intensity range. An RF frequency of 40.68 MHz is provided by the RF power generator CESAR 4040. The auto-matching network Navigator 4040 LT70 is connected RF generator to minimise the reflected power. Considering the relative high RF frequency and the dependence of the antenna impedance on the operative frequency, the dimensions of the antenna are quite reduced, if compared to the IPG6-S. Since the RF power coupling efficiency depends on the antenna parameters, in order to relax the constraints on the antenna dimensions and impedance, a modification of the matching network is required. A capacitor is foreseen to be connected to the auto-matching network to increase the maximum allowable load impedance.

7. Conclusions

Within the EU-funded Horizon 2020 DISCOVERER project, IRS is developing an IPT for an Atmosphere-Breathing propulsion system to be applied to VLEO platforms. As test-bed of small scale inductively heated plasma generators, IPG6-S has been modified with the installation of an EM, designed according to simulations performed by HELIC and ADAMANT. The DC power supply used to fed a 800-turns cylindrical EM is capable to supply a maximum of 15A, corresponding to a B-field of more than 60mT at the centre of the EM. Based on the theory of Thomson equivalent circuit, the logic algorithm, adopted to preliminary design an efficient plasma source through HELIC, focuses on the enhancement of power transfer efficiency due the increasing plasma equivalent resistance, R_p, over antenna resistance. HELIC has demonstrated that IPG6-S can be improved, but also highlighted the strong dependence of the unmagnetized source on plasma parameters, mostly T_e, ν, p, for a given plasma density. The main advantage of the application of an external B_0-field is that RF power is absorbed by plasma even in conditions of low p, T_e and ν, since collisionless mechanisms take place in the discharge. Thanks to a collaboration established between IRS and "Università degli Studi di Padova", IPG6-S has been numerically investigated through ADAMANT, a Fortran code which has been primary developed for the study of wave propagation and for the design and optimization of antennas. Indeed, the validation of IPG6-S model developed in HELIC has been necessary because of the hypothesis of infinitely thin antenna implemented in the code. Investigations in ADAMANT highlight the strong dependence of plasma absorptivity on the complex RF input power and electrical parameters of the electrical circuit. Briefly, ADAMANT and HELIC have estimated with good agreement the response of P_p on plasma parameters: in case of unmagnetized sources, both codes have predicted an increasing of the power coupling efficiency for higher p and T_e; a decreasing trend of P_p with the increasing of p and an almost independent behaviour on T_e has been observed in magnetised sources. On the other hand, by considering antenna impedance, different behaviours have been recorded. Precisely, in HELIC, R_p maxima increase and move to higher n when a greater B_0 intensity is applied. Simulations in ADAMANT have demonstrated that the application of a higher B_0 has not always a beneficial impact on the plasma absorptivity. Indeed, early results have showed asymptotic or dropping trends of $P_p(B_0)$. This was also confirmed by the experimental testing campaign. First tests of the IPG6-S/EM assembly have successfully demonstrated that the application of B_0 is advantageous in terms of:

- plasma ignition for low RF input power and low mass flow rate;
- amplification of plasma absorbed power;
- reduction of reflected power;
- confinement of the plasma plume.

Also at relatively low B_0-field, an increase of P_{RF} has been recorded. However a saturation point, after which a higher B_0-field does not influence the active component of P_{RF}, has been found. Within the framework of this paper, plasma parameters have been evaluated according to literature, but, for the design of the IPT, plasma diagnostics is highly recommended.

The future IPT will be installed to a new facility set-up to allow plasma investigations. A first prototype for IPT has been designed and almost completely assembled. f=40.68MHz is provided by the RF power generator CESAR 4040 400. An auto-matching network, Navigator 4040 LT70, modified to increase the maximum allowable load impedance, is connected to the RF generator to minimise the reflected power. The preliminary IPT design is based on the same discharge channel dimensions of the IPG6-S.

Acknowledgments

This project has received funding from the European Union's Horizon 2020 research and innovation programme under grant agreement No. 737183. This reflects only the author's view and the European Commission is not responsible for any use that may be made of the information it contains.

Bibliography

[1] F. Romano, B. Massuti-Ballester, T. Binder, G. Herdrich, S. Fasoulas, and T. Schönherr, "System analysis and test-bed for an atmosphere-breathing electric propulsion system using an inductive plasma thruster," *Acta Astronaut.*, vol. 147, pp. 114–126, 2018.

[2] F. Romano, G. Herdrich, S. Fasoulas, T. Schönherr, N. Crisp, S. Edmondson, S. J. Haigh, R. E. Lyons, V.T.A. Oiko, P. Roberts, K. L. Smith, J. Becedas, G. González, I. Vázquez, Á. Braña, K. Antonini, K. Bay, L. Ghizoni, V. Jungnell, J. Morsbøl, T. Binder, A. Boxberger, D. G. Almiñana, S. Rodriguez-Donairee, D. Katariaf, M. Davidson, R. Outlaw, B. Belkouchi, A. Conte, J. S. Perez, R. Villain, B. Heißereri, A. Schwalber "Performance Evaluation of a Novel Inductive Atmosphere-Breathing EP system", 35th International Electric Propulsion Conference, Georgia USA, 2017.

[3] F. Romano, G. Herdrich, T. Binder, A. Boxberger, C. Traub, S. Fasoulas, T. Schönherr, P. Roberts, K. Smith, S. Edmondson, S. Haigh, N. Crisp, V. T. A. Oiko, R. Lyons, S. D. Worrall, S. Livadiotti, J. Becedas, G. Gonzalez, R.M. Dominguez, L. Ghizoni, V. Jungnell, K. Bay, J. Morsbøl, D. G. Almiñana, S. Rodriguez-Donaire, M. Sureda, D. Kataria, R. Outlaw, R. Villain, J. S. Perez, A. Conte, B. Belkouchi, A. Schwalber, B. Heißerer, "Effects of applied magnetic field on IPG6-S , test-bed for an ABEP-based inductive plasma thruster (IPT)," Space Propuls. 2018, Seville, Spain, 2018.

[4] P. Chabert and N. Braithwaite, *Physics of Radio-Frequency Plasmas*. Cambridge University Press, 2011.

[5] P. C. E. Roberts, N. H. Crisp, S. Edmonson, D. García-Almiñana, S. Rodríguez Donaire, S. Haigh, R. Lyons, V. Oiko, A. M. Rojas, K. Smith, J. Becedas, G. Gonzalez, I. Vasquez, A. Brana, K. Antonini, K. Bay, L. Ghizoni, V. Jungnell, J. Morsbol, T. Binder, A. Boxberger "DISCOVERER - Radical Redesign of Earth Observation Satellites for Sustained Operation at Significantly Low Altitudes," 68th International Astronautical Congress 2017, Adelaide, Australia, 25-29 September 2017.

[6] T. Misuri, C. Ducci, R. Albertoni, M. Andreucci, "SITAEL Low-Power Hall Effect Thrusters for Small Satellites." Joint Conference of 30th International Symposium on Space Technology and Science 34th International Electric Propulsion Conference and 6th Nano-satellite Symposium, Hyogo-Kobe, Japan, July 4-10, 2015.

[7] J. Schmidt, G. Herdrich, T. W. Hyde, and R. Laufer, "Characterization and application of the inductively-heated plasma generator IPG6-B," in *Bulletin of the American Physical Society*, Portland, Oregon.

[8] M. W. Winter, "Low Power Plasma Facilities for the Investigation of Gas-Surface Interaction at the University of Kentucky," presented at the 53rdAIAA Aerospace Sciences Meeting, Kissimmee , Florida.

[9] D. Arnush, "The role of Trivelpiece–Gould waves in antenna coupling to helicon waves," *Phys. Plasmas*, vol. 7, no. 7, pp. 3042–3050, Jun. 2000.

[10] D. Arnush and F. F. Chen, "Generalized theory of helicon waves. II. Excitation and absorption," *Phys. Plasmas*, vol. 5, no. 5, p. 1239, 1998.

[11] F. F. Chen and D. Arnush, "Generalized theory of helicon waves. I. Normal modes," *Phys. Plasmas*, vol. 4, no. 9, pp. 3411–3421, 1997.

[12] D.Melazzi and V.Lancellotti, "ADAMANT: A surface and volume integral-equation solver for the analysis and design of helicon plasma sources," *Comput. Phys. Commun.*, vol. 185, no. 7, pp. 1914–1935, Jul. 2014.

[13] F. Romano, G. Herdrich, A. Boxberger, P.C.E. Roberts, S. Rodriguez-Donaire, D. Garcia-Almiñana, M. Sureda, N. H. Crisp, S. Edmondson, S.Haigh, R.E. Lyons, V.T.A. Oiko, K. Smith,S. Livadiotti, J. Becedas, G. González, R.M. Dominguez, L. Ghizoni, V. Jungnell, K. Bay, J. Morsbøl, T. Binder, C. Traub, S. Fasoulas, D. Kataria, R. Outlaw, R. Villain, J.S. Perez, A. Conte, B. Belkouchi, B. Heißerer, A. Schwalber, "Advances on the Inductive Plasma Thruster Design for an Atmosphere-Breathing EP System" in *International Astronautical Congress IAC 2018*, Bremen, Germany, 1-5 October 2018.

[14] M. Dropmann, G. Herdrich, R. Laufer, D. Puckert, H. Fulge, S. Fasoulas, J. Schmoke, M. Cook, T. W. Hyde, "A New Inductively Driven Plasma Generator (IPG6)—Setup and Initial Experiments," *IEEE Trans. Plasma Sci.*, vol. 41, no. 4, pp. 804–810, Apr. 2013.

[15] F. F. Chen, *Introduction to Plasma Physics and Controlled Fusion*, 3rd ed. Springer International Publishing, 2016.

[16] Georg Herdrich, Dissertation: „Aufbau, Qualifikation und Charakterisierung einer induktiv beheizten Plasmawindkanalanlage zur Simulation atmosphärischer Eintrittsmanöver", Institut für Raumfahrtsysteme, Universität Stuttgart, URN: urn:nbn:de:bsz:93-opus-21478,URL:http://elib.uni-stuttgart.de/opus/volltexte/2005/2147/, and in extended print run with Shaker Publishing Company ISBN 3-8322-4338-0, Dec. 2004

[17] S. J. J. Thomson, "The electrodeless discharge through gases," *Proc. Phys. Soc.*, vol. 40, no. 1, p. 79, 1927.

[18] F. F. Chen, “Permanent Magnet Helicon Source for Ion Propulsion,” *IEEE Trans. Plasma Sci.*, vol. 36, no. 5, pp. 2095–2110, Oct. 2008.

[19] E. A. Kral’kina, “Low-pressure radio-frequency inductive discharge and possibilities of optimizing inductive plasma sources,” *Phys.-Uspekhi*, vol. 51, no. 5, p. 493, 2008.

[20] G. Herdrich, M. Auweter-Kurtz, H. L. Kurtz, T. Laux, and M. Winter, “Operational Behavior of Inductively Heated Plasma Source IPG3 for Entry Simulations,” *J. Thermophys. Heat Transf.*, vol. 16, no. 3, pp. 440–449, Jul. 2002.

[21] E. A. Kralkina, A. A. Rukhadze, V. B. Pavlov, K. V. Vavilin, P. A. Nekliudova, A. K. Petrov and A. F. Alexandrov, “RF power absorption by plasma of a low-pressure inductive discharge,” *Plasma Sources Sci. Technol.*, vol. 25, no. 1, p. 015016, 2016.

[22] F. F. Chen, “The low-field density peak in helicon discharges,” *Phys. Plasmas*, vol. 10, no. 6, pp. 2586–2592, May 2003.

[23] D. D. Blackwell, T. G. Madziwa, D. Arnush, and F. F. Chen, “Evidence for Trivelpiece-Gould Modes in a Helicon Discharge,” *Phys. Rev. Lett.*, vol. 88, no. 14, p. 145002, Mar. 2002.

[24] “Finite Element Method Magnetics: Documentation.” [Online]. Available: http://www.femm.info/wiki/Documentation/. [Accessed: 21-Oct-2018].